Symbiosis of different-sized drops

I. Leizerson,[1] S. G. Lipson,[1] and A. V. Lyushnin[2]
[1]*Department of Physics, Technion–Israel Institute of Technology, 32000 Haifa, Israel*
[2]*Department of Theoretical Physics, Perm State Pedagogical University, Perm 614600, Russia*
(Received 26 March 2003; published 20 November 2003)

We demonstrate that the usual situation of coarsening in crystal growth or Ostwald ripening in evaporating liquid drops is not universal, and when the drops coexist with a microscopically thin continuous surface film, a different behavior is observed. The predicted behavior was investigated experimentally and supported by numerical simulations.

DOI: 10.1103/PhysRevE.68.051601 PACS number(s): 68.15.+e, 47.54.+r, 64.70.Fx, 68.03.Cd

INTRODUCTION

An ensemble of volatile liquid drops is generally in unstable equilibrium with its vapor because of the Gibbs-Thomson effect. Just above the equilibrium vapor pressure over a flat surface, large drops grow at the expense of smaller ones, whereas below it all drops evaporate, the smallest drops fastest. The same is true of drops in contact with vapor on a partially wetted substrate of given contact angle. However, we have noticed that an array of variously sized water drops on a clean mica substrate behaves differently [1]; above the equilibrium vapor pressure the mica is completely wet, whereas below it the largest drops evaporate fastest, and an approximately stable drop distribution is attained with a slowly decreasing scale parameter. We attribute this behavior to an interaction between the surface and the fluid involving two antagonistic forces, which predicts complete wetting under saturated vapor pressure, but an equilibrium between macroscopic drops and a very thin continuous layer of water covering the substrate under subsaturated conditions. Measurements of the two film thicknesses and the transition region between them are presented. In this case the concepts of contact line and angle are not really valid. Since the film thickness is found to vary smoothly and continuously between the two thicknesses there is no substrate-liquid-vapor coexistence line. The interpretation is borne out by simple measurements of drop radii and their rate of change and also by computer simulations.

THEORY

A cleaved mica surface is known to be wetted by water; under saturated vapor pressure, a uniform macroscopically thick film of water covers the surface completely. As this water evaporates, it breaks up into interesting patterns which were predicted theoretically by Cazabat [2] and Brochard-Wyart [3], and have been demonstrated experimentally as resulting from antagonistic van der Waals and polar surface forces between the water and the substrate [4,5]. It was shown that under unsaturated conditions, a thermodynamic potential involving the film thickness analagous to the Gibbs free energy can be defined for such a system. For a range of surface force parameters, this potential has minima at two different film thicknesses. One minimum corresponds to a molecularly thin film and the second to a macroscopically thick film. Phase equilibrium between the two films is similar to that between liquid and solid, for example, and a first-order phase transition between them occurs. When a film-thickness evolution equation is written down for such a system, it approximates at different rates of evaporation to diffusion-limited solidification or viscous fingering [5]. Indeed, the dendritelike patterns which develop during evaporation were shown to be remarkably similar to those calculated for solidification in an isotropic two-dimensional system [6–8].

After a long time, the quasiequilibrium state consists of an array of drops of widely differing sizes (Fig. 1). Following this, one would then expect coarsening to occur, in which the larger drops grow at the expense of the smaller ones [9], or cooperative evaporation [10], in which larger drops acquire fluid from smaller ones through vapor transport. This was indeed observed during evaporation from a nonwetted substrate by McHale *et al.* [11], but does not happen in this case. Instead, we have observed that all the drops continue to evaporate together, and the smaller ones even evaporate more slowly than the large ones. This contrasts with the behavior of a drop array on a partially wetted surface with a

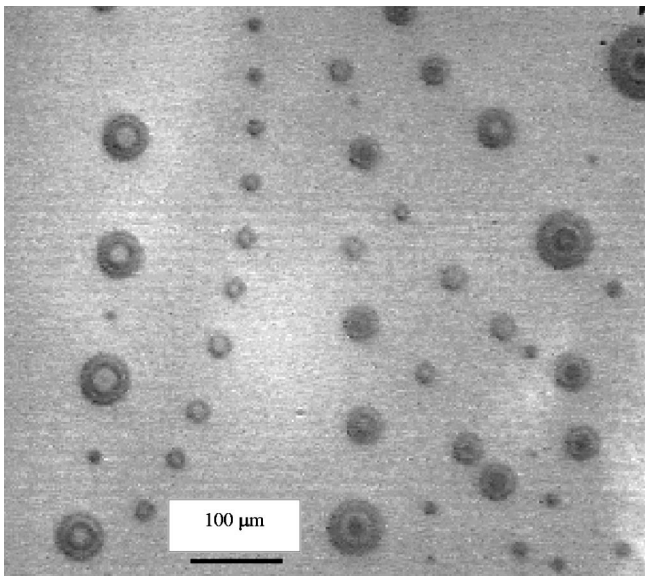

FIG. 1. An array of water drops of widely differing sizes on a mica substrate, photographed using interference contrast. The first dark ring appears at a thickness of 111 nm.

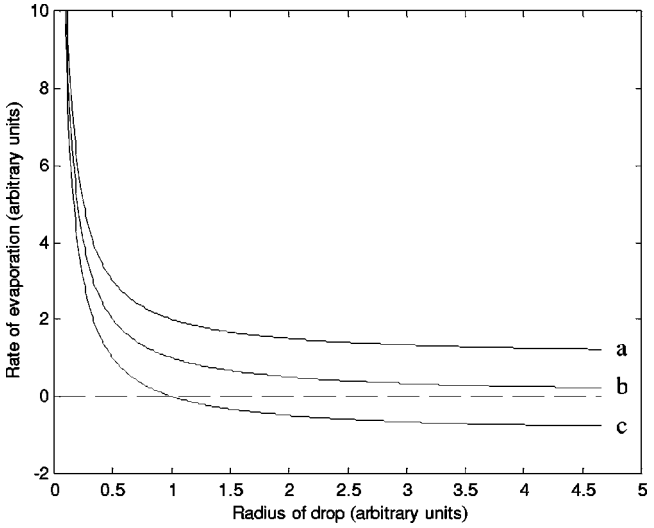

FIG. 2. The rate of evaporation of an isolated drop (negative rate of change of radius of curvature) as a function of its radius for three cases: (a) $p_{\mathrm{vap}}<p_{\mathrm{sat}}$, (b) $p_{\mathrm{vap}}=p_{\mathrm{sat}}$, (c) $p_{\mathrm{vap}}>p_{\mathrm{sat}}$. In (a) and (b) all drops evaporate; in (c) small drops evaporate and large drops grow.

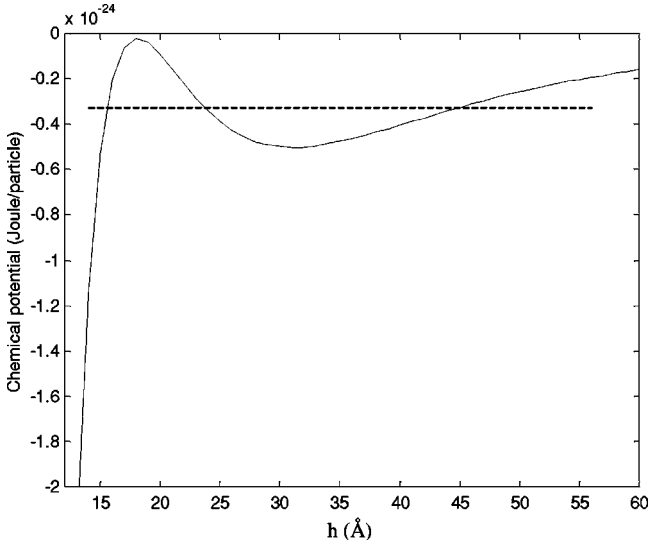

FIG. 3. The chemical potential $\rho^{-1}dg/dh$ as a function of film thickness h, according to Eq. (1). The values of the spreading coefficients are from Ref. [4]. The dashed line shows the Maxwell construction, at which the thick and thin films are in equilibrium.

defined contact angle, in which case a drop with a smaller radius of contact with the substrate (which we shall call its ''projection radius'') has a larger curvature, and therefore must evaporate faster due to the Gibbs-Thomson contribution to its vapor pressure. We attribute the observed behavior to the continuous film of molecular thickness on the mica surface, which connects the drops.

In order to emphasize the difference between the behavior of a drop assembly on a dry surface (which behaves similarly to a collection of three-dimensional drops coexisting with vapor) and the present situation, we first show the way in which the former assembly evaporates. A drop with projection radius r is the cap of a sphere having radius of curvature $R=r/\sin\theta$, where θ is the contact angle. The rate of evaporation of a drop can be assumed to be proportional to the difference between the vapor chemical potential $\mu_{\mathrm{vap}}=kT\ln(p/p_s)$, and that of the drop, $\mu_{\mathrm{drop}}=\mu_{\mathrm{liq}}+2\rho^{-1}\gamma/R$, where γ is the liquid-vapor surface tension, ρ is the density of particles in the liquid phase, p is the vapor pressure, and p_s is its saturated value. At the liquid-vapor equilibrium ($p=p_s$) we define $\mu_{\mathrm{liq}}=\mu_{\mathrm{vap}}=0$, so that drops of any finite radius evaporate, since $\mu_{\mathrm{drop}}>\mu_{\mathrm{vap}}$. At slightly higher pressure, where μ_{vap} is positive, small drops with small R evaporate, whereas larger drops with large R grow. Thus the large drops swallow up the small ones, and coarsening occurs (Fig. 2).

The excess Gibbs free energy per unit area between a polar fluid and a polar substrate has been described schematically by de Gennes [12] and an explicit formula has been given by Sharma and Jameel [4] based on experimental data by Israelachvili [13] as

$$g(h)=S^{\mathrm{LW}}/h^2+S^P\exp[(d_0-h)/l], \tag{1}$$

where S^{LW} and S^P are spreading pressures due to van der Waals and polar interactions, l is a screening length, and d_0 the molecular diameter. Figure 3 shows $\mu_{\mathrm{film}}=\rho^{-1}dg/dh$ as a function of h for typical values of the interaction parameters [4]. Three-phase equilibrium between two films and the vapor is determined by a Maxwell construction on the $\mu(h)$ diagram.

Now, consider the situation when the thick regions have shrunk to drops, connected by the thin film. The drops, whose free surface is far from the substrate, have excess chemical potential $\rho^{-1}2\gamma/R$. For equilibrium with the continuous thin film, it follows that R must be the same for all the drops, independent of their projection radii. This would seem to imply a contact angle increasing with the projection radius, which is at odds with the usual concept of a constant contact angle. But because the film is continuous, the meeting between liquid, vapor and substrate which defines the edge of a drop is not present, and so a contact angle is not defined in the conventional manner. Sharma, in simulations for such problems [14,15], defines the contact angle as the largest slope in the drop profile near the substrate, and indeed found that the angles defined in this way for drops increase monotonically with the drop volume.

What happens when a drop evaporates? Water evaporates from the spherical cap of curvature radius R and the volume is compensated by contraction of the projection radius. A balance of volumes gives a contraction velocity $v=-dr/dt$,

$$2\pi rv(h_2-h_1)=2\gamma\rho^{-1}\alpha\pi r^2/R, \tag{2}$$

in which α is the rate of evaporation per difference in chemical potential between the bulk and the vapor. It is important to emphasize that there is no evaporation at the edge because its profile is in equilibrium with the unsaturated vapor. Remembering that R is the same for all the drops, one immediately sees that dr/dt is proportional to $-r$.

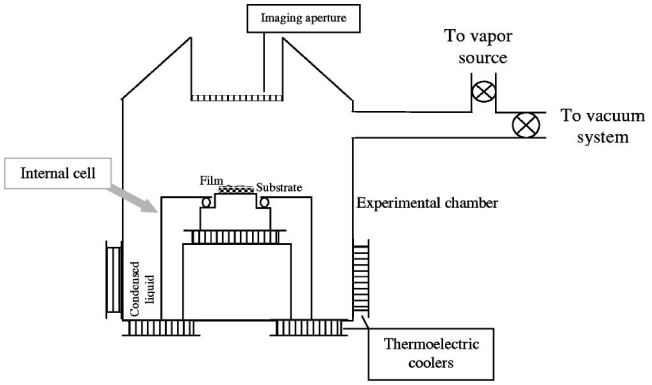

FIG. 4. Experimental setup.

EXPERIMENTS

Measurements of the drop diameters and radii of curvature as a function of time were made on video recordings of interference micrograms (e.g., Fig. 1) of drops. The experiments were carried out at 0 °C in a system (Fig. 4) evacuated to a high vacuum, into which water vapor could be introduced by evaporation from a separate chamber containing distilled water [17]. The temperature T of the copper experimental cell is controlled by an arrangement of thermoelectric coolers. The mica sample under investigation is attached by a thin layer of high-vacuum black wax to a copper pedestal in the form of a ring, so that part of the mica is free standing. The sample and pedestal temperature T_s is controlled independently by an additional thermoelectric cooler. If $T_s < T$, water vapor condenses from the cell walls to the sample surface; if $T_s > T$, the opposite occurs. Mica substrates are prepared by cleavage *in situ* and then exposed to water vapor only. The cleavage is carried out by attaching an iron piece to the upper mica surface. Then a strong magnet brought close from outside the cell tears away the iron piece together with a layer of mica, leaving a fresh clean surface.

The pattern created the on mica surface is observed by a $10\times$ magnification reflective microscope with numerical aperture (NA) of 0.1. Illumination by a Hg lamp with a filter to isolate the $\lambda = 546$ nm line gives a coherence length of about 1 mm, enough to produce the necessary combined interferometric image involving both mica surfaces. The radii of curvature R are measured using interference rings on drops thicker than $\lambda/2n$. Figure 5 shows that the measured R is independent of r, but decreases slowly with time, the larger drops evaporating faster. It can be compared to a similar experiment at the same p/p_{sat} on nonwetting mica (after exposure to humid air for a long period) in which small drops were swallowed by big ones within 30 s. The film profile shown in Fig. 6 was measured using the technique of three-beam interferometry, involving reflections at the vapor-film interface and both mica surfaces [16]. It shows quantitatively the thickness of the two films predicted by the model; the two films are separated by a higher rim, which develops due to hydrodynamic flow, and has been seen previously in both experiments [5,17] and simulations [14,15,18]. It can be seen that for the case investigated the two films are 25 ± 5 and 110 ± 10 Å thick. It should be pointed out that these measurements are relative to ''clean mica'' under the lowest vapor pressure attainable in the system, which would still be covered by a monolayer of water [19]. The mica thickness is chosen so that the superposition of the reflected waves from its two surfaces is in quadrature with the wave reflected from the water surface. This means that the total light intensity reflected varies linearly with h when $h \ll \lambda$. This should be compared to conventional interference between the top and bottom of the water film, for which the light intensity varies quadratically with the thickness when $h \ll \lambda$, and is therefore insensitive to very thin films. By carefully choosing the thickness of the mica, which involves considerable trial and error since a further cleavage was sometimes performed after mounting the sample, the method can be used to determine film thickness down to 5 Å, limited by noise in the imaging and the number of bits in the charge-coupled device camera.

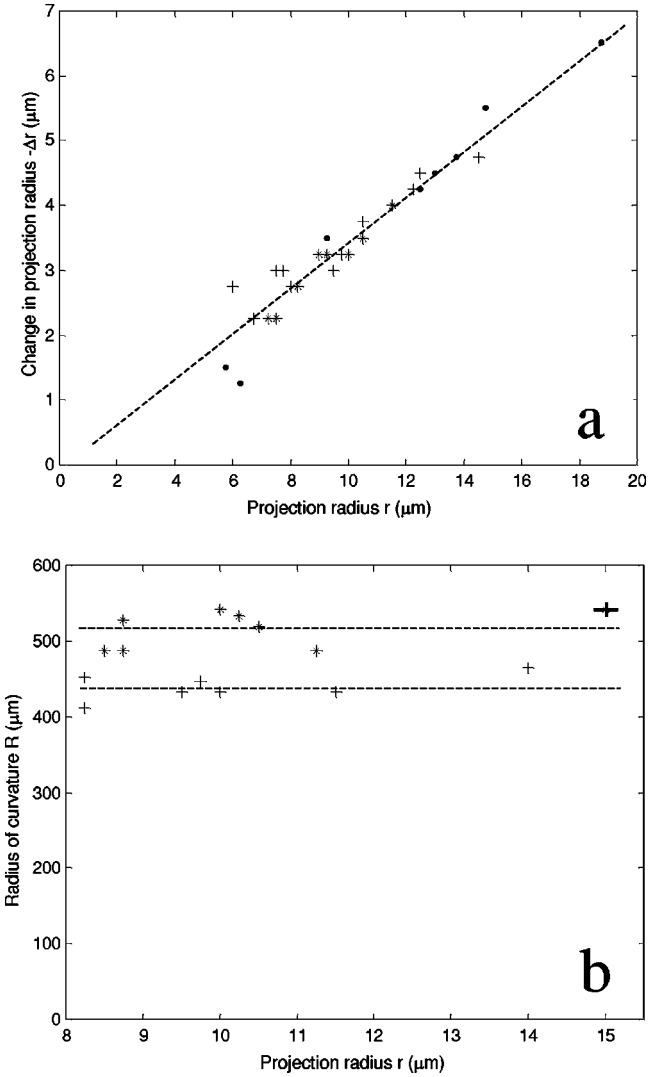

FIG. 5. (a) The change in projection radius of drops during 15 min as a function of their radius, for three different experiments under the same conditions, $p/p_{\mathrm{sat}} = 0.920 \pm 0.002$. The linear relationship is clear. (b) Radius of curvature of the larger drops is independent of their projection radius. The two lines refer to the same field of drops at different times. Typical error bar is shown on one point.

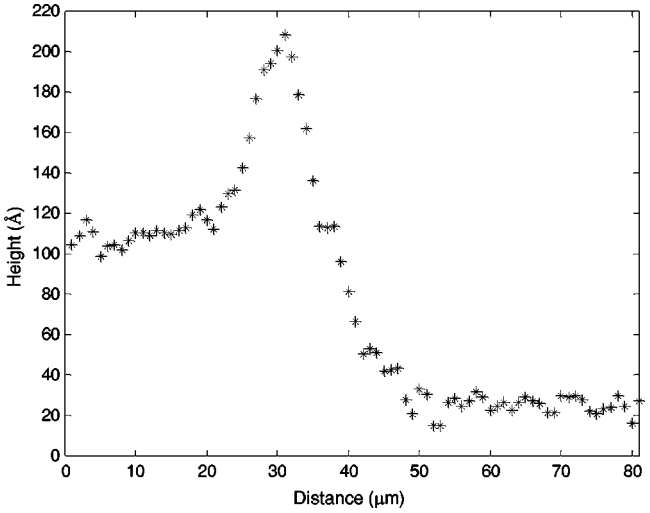

FIG. 6. Profile of the interface between the thin and thick films, measured by three-beam interferometry. The higher rim is a hydrodynamic phenomenon which appears because of flow when the edge is moving.

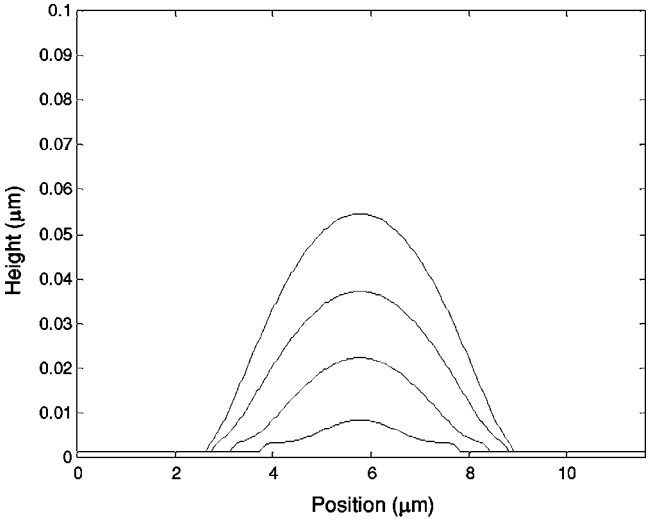

FIG. 7. A calculated drop profile. The existence of a step near the edge of the drop should be noticed. The great difference between the height and width scales makes a spherical drop look parabolic.

COMPUTATIONAL SIMULATIONS

The dynamic equation proposed to describe the volatile thin film rupture towards equilibrium is the following [5]:

$$\frac{\partial h}{\partial t} = \nabla \cdot \left[\frac{h^3}{3\eta} \nabla \left(\frac{dg}{dh} - \gamma \nabla^2 h \right) \right] - \frac{\alpha}{\rho} \left(\frac{dg}{dh} - \gamma \nabla^2 h - \rho \mu_{\text{vap}} \right), \tag{3}$$

where η is the viscosity, $\mu_{\text{vapor}} = k_B T \ln(p/p_s)$ is the chemical potential of water vapor, ρ is the density of molecules in water, and α is an evaporation constant. This equation was solved numerically for conditions similar to experimental ($p/p_s = 0.95$, causing evaporation of the thick uniform water film at rate of 7 nm/s) and based on the potential g described above. This was calculated by a standard Crank-Nicholson method of finite differences [18] with boundary conditions $h_x = h_{xxx} = 0$ on both ends of the computational interval. The system of nine linear equations was solved by use of Stone's algorithm. The cross section of an evaporating drop is shown by Fig. 7, which is the result of a simulation for the type of surface interaction described above [18]. The important point to emphasize is that the profile of the edge of the drop is controlled by the interaction with the substrate, and the continuous film changes from h_1 to h_2 in a short distance (forming a step which is in equilibrium with the vapor). This joins continuously to the spherical cap of the drop, which for the most part is sufficiently remote to be unaffected by the presence of the substrate.

SUMMARY

The experiments showed that the usual situation of large drops in an array growing at the expense of small ones is not universally observed, and when the drops coexist with a microscopically thin continuous surface layer, a different behavior is observed.

ACKNOWLEDGMENTS

We thank S. Hoida for technical assistance and D. S. Tannhauser for critically reading the manuscript. This work was supported by the Minerva Foundation for Non-linear Science and the Technion V. P. fund for the Promotion of Research.

[1] I. Leizerson, S. G. Lipson, and A. V. Lyushnin, Nature (London) **422**, 395 (2002).
[2] A.-M. Cazabat, Contemp. Phys. **28**, 347 (1987).
[3] F. Brochard-Wyart, *Soft Matter Physics*, (Springer, Berlin, 1995), pp. 7–44.
[4] A. Sharma and A. Jameel, J. Colloid Interface Sci. **161**, 190 (1993).
[5] N. Samid-Merzel, S. G. Lipson, and D. S. Tanhauser, Phys. Rev. E **57**, 2906 (1998).
[6] E. Ben-Jacob, Contemp. Phys. **34**, 247 (1993).
[7] E. Ben-Jacob, Nature (London) **343**, 523 (1990).
[8] T. Ihle and H. Muller Krumbhaar, Phys. Rev. Lett. **70**, 3083 (1993).
[9] A. W. Adamson, *Physical Chemistry of Surfaces* (Wiley-Interscience, New York, 1997).
[10] C. Schafle, C. Bechinger, B. Rinn, C. David, and P. Leiderer, Phys. Rev. Lett. **83**, 5302 (1999).
[11] G. McHale, S. M. Rowan, M. I. Newton, and M. K. Banerjee, J. Phys. Chem. B **102**, 1964 (1998).
[12] P. G. de Gennes, Rev. Mod. Phys. **57**, 325 (1985).
[13] J. Israelachvili, *Intermolecular and Surface Forces*, 2nd ed. (Academic, San Diego, 1992).

[14] A. Sharma, Langmuir **9**, 3580 (1993).
[15] A. Sharma, Langmuir **14**, 4915 (1998).
[16] I. Leizerson and S. G. Lipson, Appl. Phys. Lett. **83**, 260 (2003).
[17] M. Elbaum and S. G. Lipson, Phys. Rev. Lett. **72**, 3562 (1994).
[18] A. V. Lyushnin, A. A. Golovin, and L. M. Pismen, Phys. Rev. E **65**, 021602 (2002).
[19] D. Beaglehole and H. K. Christenson, J. Phys. Chem. **96**, 3395 (1992).